Divergence of seafloor elevation and sea level rise in coral reef regions

Kimberly K. Yates[1], David G. Zawada[1], Nathan A. Smiley[1], Ginger Tiling-Range[2]

[1]U.S. Geological Survey, Coastal and Marine Science Center, 600 Fourth St. South, St. Petersburg, Florida 33701, U.S.A.
5   [2]Cherokee Nation Technologies as contracted to the U.S. Geological Survey, 600 Fourth St. South, St. Petersburg, Florida 33701, U.S.A.

Correspondence to: Kimberly K. Yates (kyates@usgs.gov)

Abstract. Coral reefs serve as natural barriers that protect adjacent shorelines from coastal hazards such as storms, waves
10   and erosion. Projections indicate global degradation of coral reefs due to anthropogenic impacts and climate change will
cause a transition to net erosion by mid-century. Here, we provide a comprehensive assessment of the combined effect of all
of the processes affecting seafloor accretion and erosion by measuring changes in seafloor elevation and volume for 5 coral
reef ecosystems in the Atlantic, Pacific and Caribbean over the last several decades. Regional-scale mean elevation and
volume losses were observed at all 5 study sites and in 78% of the 59 individual habitats that we examined across all study
15   sites. We estimate that 12% to 65% of seafloor elevation loss may be attributed to reduced carbonate production, bioerosion
and carbonate dissolution and 35% to 88% may be attributed to physical erosion and export of sediment from these systems.
Erosion of both coral-dominated substrate and non-coral substrate suggests that the current rate of carbonate production is no
longer sufficient to support net accretion of coral reefs or adjacent habitats. We show that regional-scale loss of seafloor
elevation and volume has accelerated the rate of relative sea level rise in these regions. Current water depths have increased
20   to levels not predicted until near the year 2100, placing these ecosystems and nearby communities at elevated and
accelerating risk to coastal hazards. Our results set a new baseline for projecting future impacts to coastal communities
resulting from degradation of coral reef systems and associated losses of natural and socio-economic resources.

1 Introduction

Coral reef ecosystems develop over thousands of years as organisms build skeletons of calcium carbonate minerals that form
25   complex 3-dimensional structures, and keep pace with rising sea level through continued growth and accretion of carbonate
sediments. These ecosystems support up to 25% of fisheries in tropical regions and developing nations (Garcia and Moreno,
2003), and economic and recreational services for more than 100 countries (Burke et al., 2011). Reef framework and
shallow, non-coral-dominated habitats serve as natural barriers that protect shoreline ecosystems and coastal communities by
reducing hazards from waves, storm surges and tsunamis for more than 200 million people around the world (Sheppard et
30   al., 2005; Ferrario et al., 2014). Local and global, natural and human-induced stressors have caused the loss of reef-building

organisms and reef structure, a decrease in biodiversity, a transition to algal-dominated communities (Pandolfi et al., 2003), and an increase of bioerosion (Alvarez-Filip et al., 2009), placing coral reefs around the world in a state of rapid decline (Madin and Madin, 2015).

5   Coral reef degradation and the causes have been well documented since the 1970's (Gardner et al., 2003) when regional-scale species compositions that remained stable throughout the Pleistocene and Holocene began changing (Aronson et al., 2002). Most reef degradation has been attributed primarily to impacts of coastal development, overfishing, pollution, nutrient enrichment, coral bleaching and disease (Glynn, 1984; Greenstein et al., 1998). Abundance of reef-building corals has decreased as much as 72% since 1968 on Pacific reefs and as much as 50% since 1970 on many Caribbean reefs (Gardner et
10   al., 2003; Bruno and Selig, 2007; 2014; Jackson et al., 2014). Carbonate production rates have decreased to below historical values on Caribbean reefs and carbonate-budget models indicate that some are already experiencing net erosion (Perry et al., 2013). Projections indicate up to 66% of coral reefs worldwide will continue to degrade in the next few decades due to ocean warming and acidification from unprecedented rates of global climate change (Frieler et al., 2013) that may cause reef erosion to exceed accretion (Hoegh-Guldberg et al., 2007). Ancient reef crises linked to global climate change during the
15   past 500 million years are marked in the geologic record by major decreases in carbonate accretion and reef volume (Kiessling and Simpson, 2011).

Numerous studies have modeled reef- to regional-scale accretion and erosion on coral reefs based solely on carbonate budgets some of which account for rates of bioerosion (Stearn, 1977; Brock, 2006; Moses, 2009; Kennedy et al., 2013; Leon,
20   2013a; Perry et al., 2013; Perry et al., 2014; Perry, 2015). Recent studies have also measured regional-scale chemical erosion of carbonates due to dissolution caused by ocean acidification (Brock, 2006; Moses, 2009; Muehllehner, 2016). Very few studies have quantified sediment transport and export on reef systems (Kench, 2004; Morgan, 2014). Such studies are essential for attributing ecosystem change to cause, setting target levels for restoring and maintaining healthy reefs (Kennedy et al., 2013) and for measuring and predicting reef degradation due to these specific process rates. However, no prior studies
25   provide a comprehensive assessment of total seafloor elevation and volume change due to the combined effect of all of the processes affecting seafloor accretion and erosion (i.e., including physical erosion; redistribution, import or export of seafloor sediments; compaction; direct human alterations to the seafloor, carbonate production, bioerosion, chemical erosion). Vertical accretion or erosion of coral reef ecosystems is a function of total mass balance (Schlager, 1981). Therefore, measures of total system change in seafloor elevation and volume are required to accurately assess and predict the
30   impact of reef degradation on the vulnerability of coastal communities to hazards caused by storms, waves, sea level rise and erosion.

Here, we quantify the combined effect of all constructive and destructive processes on modern coral reef ecosystems by measuring regional-scale changes in seafloor elevation. We assessed 5 coral reef ecosystems in the Atlantic (Upper and

Lower Florida Keys), Caribbean (U.S. Virgin Islands), and Pacific (Maui, Hawaii) including both coral-dominated habitats and adjacent, non-coral dominated habitats. We adapted an elevation-change analysis method that has traditionally been used to monitor seafloor changes such as sediment accretion and erosion, and migration of shipping channels, sand bars, mud banks and other seafloor features in coastal environments (Byrnes et al., 2002; Taylor and Purkis, 2012; Byrnes et al., 2013)

5 and we present results from the first application of this method to coral reef ecosystems. We used historical bathymetric data from the 1930's to 1980's and contemporary Light Detection and Ranging (LiDAR) digital elevation models (DEMs) from the late 1990's to 2000's to calculate changes in seafloor elevation for each study site (Tables S1 & S2) over time periods reflecting low to high anthropogenic impact (Table S3). We then created elevation-difference models from which we calculated corresponding changes in seafloor volume for whole study sites and for habitat types within each site. The

10 magnitude of erosion that has already occurred, trajectories for continued coral reef degradation (Kennedy et al., 2013) and increasing sea level place these ecosystems and nearby communities at elevated and accelerating risk to coastal hazards.

2 Methods

2.1 Geospatial transformation of historical and LiDAR bathymetric soundings

Our selection of study sites was based on the availability of historic bathymetry that was collocated with recent Light

15 Detection and Ranging (LiDAR) elevation data, had sufficient point density and geospatial information to support meaningful comparisons with LiDAR data, and spanned low to high anthropogenic impact time periods. We defined relative anthropogenic impact based on the simplest first-order parameter of population. Low anthropogenic impact (historic data or geographic area) was defined as having a population of approximately half or less of recent time periods or uninhabited geographic area (Table S3). Population data was acquired from the U.S. Census Bureau (U.S. Census Bureau). Full analysis

20 of anthropogenic impact factors (e.g., urban extent, developed land, terrestrial water run-off, water quality, etc.) is beyond the scope of this paper.

Historical hydrographic survey (H-sheet) data collected by the United States Coast and Geodetic Survey (USC&GS) or the National Ocean Service (NOS) between 1934 and 1982, including descriptive reports, digital XYZ sounding data and

25 smooth sheets, were downloaded from National Oceanic and Atmospheric Administration's (NOAA) Office of Coast Survey (NOAA Office of Coast Survey). The number of H-sheets used for each study site varied from 1 to 24 depending on geographic area. All data sources and descriptions are listed in Table S1. The historical sounding data for Buck Island and Maui were reported to the nearest tenth of a fathom (18 cm) for water depths less than 20 fathoms (37 m) and 11 fathoms (20 m), respectively, and to the nearest 1 fathom (1.8 m) for greater water depths. Therefore, we only used data from shallower

30 depths than these thresholds at these study sites.

Sounding position for 1930's data was determined by sextant triangulations using both permanent and temporary

topographic reference points or triangulation stations, theodolite fixes, navigational beacons, and ship time and speed fixes (Shalowitz, 1964). Sounding data that was downloaded from the NOAA website for use in our study had already been digitized by personnel at NOAA. Vertical units for the original soundings remained in their original vertical datum, but were converted from feet and fathoms to meters by NOAA. We determined vertical datums for the digitized soundings by

5   reviewing the smooth sheet notes and descriptive reports. NOAA also converted horizontal datums of the digital XYZ soundings to North American Datum 1983 (NAD83) during the digitization process.

Comparison between historical and modern sounding data sets required conversion to a common vertical datum. We adjusted data using NOAA relative sea level rise (RSLR) estimates to account for any differences at tide stations caused by

10   sea level rise, glacial rebound, and subsidence (Parker, 1992; Byrnes et al., 2013) between time periods. Tide stations nearest to each study site, and with length of sea-level-trend data that spanned the time range of historical and modern bathymetric data sets, were chosen for acquisition of mean sea-level-trend data (Table S3). The correction factor was based on NOAA's mean sea-level-trend rate and multiplied by the time span between the year of the historical survey and the year of the modern LiDAR dataset and added to the historical sounding value.

We transformed historical sounding data from tidal datums mean low water and mean lower low water (MLW/MLLW) to a modern orthometric datum using NOAA's vertical datum transformation software (VDatum v3.6) to adjust vertical and horizontal datums to match those of corresponding modern LiDAR data. The XYZ output files were reformatted in Excel to remove unnecessary columns and add appropriate headers before importing into ESRI ArcGIS ArcMap 10.2.2 to create

20   shapefiles. Review of the smooth sheets revealed soundings from multiple time periods. The metadata associated with the digital soundings did not include information on which soundings were digitized. We georectified the smooth sheets using available North American Datum 1927 (NAD27) corrections on the smooth sheets and additional control points if necessary to determine which points were included during NOAA's digitization process. Smooth sheets georectified to NAD27 were then projected to Universal Transverse Mercator (UTM) NAD83 in ESRI ArcGIS ArcMap 10.2.2. Digital XYZ sounding

25   data were overlaid on the smooth sheets and reviewed point by point to determine and remove soundings from the shapefile (Buster and Morton, 2011) that were from earlier or later time periods. Edited digital XYZ sounding files for each smooth sheet were then merged to create a single digital XYZ sounding shapefile for each study area at the time period of interest.

LiDAR data sets (U.S. Army Corps of Engineers-JALBTCX, 1999, 2004; Brock et al., 2006; Brock et al., 2007; Fredericks

30   et al., 2015b, a) from the USGS Coastal and Marine Geology LiDAR program and the U.S. Army Corps of Engineers (USACE) Joint Airborne LiDAR Bathymetry Technical Center of Expertise (JALBTCX) were downloaded for each study site (Table S1). LiDAR digital elevation models (DEMs) for Atlantic/Caribbean and Pacific sites were at horizontal spatial resolutions of 1 m and 4 m, respectively, with horizontal datums of UTM NAD83, and vertical datums of NAVD88 GEOID03 for the Atlantic, VIVD09 for the Caribbean, and MLLW for the Pacific. We imported LiDAR datasets to ArcMap

in raster format. We used ArcMap Spatial Analyst Tools ('Extraction' > 'Extract Values to Points') and the XYZ historical point-data shapefiles to extract corresponding elevations from the LiDAR DEMs at the location of the historical points. The resulting shapefile from the historical-point to LiDAR-DEM (point-to-DEM) extraction contained fields for historical and LiDAR soundings.

2.2 Calculation of elevation change

Elevation change between historical and modern data was calculated by adding a field to the attribute table of the point-to-DEM shapefile. We then used the 'Field Calculator' to calculate the elevation differences between the historical and LiDAR soundings and created a new XYZ_{change} data set whereby Z_{change} = modern LiDAR elevation data point – historical elevation

10 data point (negative values indicate loss of seafloor elevation and positive values indicate gain of seafloor elevation). We used the XYZ_{change} data sets for elevation analysis of each study site including calculation of mean elevation change and analysis of elevation change by habitat type.

2.3 Elevation- and volume-change analysis – TIN modeling

We used a multi-step process in ArcMap to create a surface model from the XYZ_{change} points to estimate seafloor-elevation

15 and reef-volume changes. First, we created a Triangulated Irregular Network (TIN, a digital data structure used in a geographic information system (GIS) for representing a surface) from the XYZ_{change} points using the 'Create TIN' tool. TIN surface modeling of historic bathymetry data was used due to the irregular spatial distribution of these XYZ_{change} points. However, because the Delaunay triangulation algorithm used by the 'Create TIN' tool creates a comprehensive network of triangles spanning the entire dataset, some of these triangles were inapplicable to our study. For example, the XYZ_{change}

20 points for Maui form a ring around the island, however, the resultant TIN includes triangles spanning the interior of the island. We removed such triangles from each TIN using the 'Delineate TIN Data Area' tool by specifying a maximum edge length for triangulation determined for each site based on its geographic characteristics and the spacing of the XYZ_{change} points. The lengths we used were 200 m for Buck Island (BI); 400 m for the Upper Florida Keys (UFK) and St. Thomas (STT); 900 m for the Lower Florida Keys (LFK); and 1000 m for Maui. Next, we created a polygon representing the 2-

25 dimensional footprint of the TIN using the 'TIN Domain' tool. After this clipping process, smaller triangles that covered sub-aerial features (such as rock outcroppings, sand spits, and small islands) still remained in some data sets. Since the LiDAR DEMs we used contained only bathymetric surfaces, such features were not included, and we used the 2D LiDAR footprint to remove these triangles according to the following steps. We created a polygon representing the 2-dimensional footprint of the DEM using the 'Raster Domain' tool. Next, we created a new polygon representing the intersection of the

30 TIN and LiDAR footprints using the 'Clip' tool. We set the 'Input Features' parameter to the TIN footprint and the 'Clip Features' parameter to the LiDAR footprint. These parameter settings were critical for obtaining the correct result. Finally, we used the footprint-intersection polygon to remove any remaining irrelevant triangles from the TIN by applying the 'Edit

TIN' tool and the following parameter settings:

1) set 'Input Feature Class' to the footprint-intersection polygon;

2) set 'Height Field' to 'None';

3) set 'SF Type' to 'Hard Clip';

5   4) set 'Tag Field' to 'None'.

The resultant clipped TINs encompassed all XYZ_{change} points and were free of extraneous triangles. We used these clipped TINs to compute surface volumes using the 'Surface Volume' tool for 4 scenarios based on the following parameter settings:

1) net accretion – maximum bound: 'Reference Plane' set to 'ABOVE' and 'Plane Height' set to 0 m

2) net erosion – maximum bound: 'Reference Plane' set to 'BELOW' and 'Plane Height' set to 0 m

10   3) net accretion – minimum bound: 'Reference Plane' set to 'ABOVE' and 'Plane Height' set to 0.5 m

4) net erosion – minimum bound: 'Reference Plane' set to 'BELOW' and 'Plane Height' set to -0.5 m

The two 'minimum bound' cases are estimates that account for combined measurement errors (discussed in the 'Vertical error analysis' section) in both the historical sounding and LiDAR elevation data. We also used the 'Surface Volume' tool to compute the 2-dimensional footprint area of each clipped TIN by setting 'Reference Plane' to 'BELOW' and 'Plane Height'

15 to a positive value greater than the highest TIN elevation. In our study, we used a plane height of 100 m to force the algorithm to take a nadir view of the TIN.

2.3.1 Elevation- and volume-change analysis by habitat

We obtained benthic-habitat-map shapefiles (Florida Fish and Wildlife Conservation Commission, 2015) for the Upper and Lower Florida Keys study sites from Florida Fish and Wildlife Conservation Commission (FWC). The Unified Florida Reef

20 Tract (UFRT) map Version 1.2 is comprised of 5 class levels from 0 to 4. We used class level 2 for our study because the level of detail was consistent with benthic habitat data available at our other study sites. We obtained benthic-habitat-map shapefiles for the USVI and Maui from NOAA (Rohmann, 2001b, a; Battista and Christensen, 2007). We delineated USVI habitats using the 'type' descriptor in the shapefile's attribute table. We delineated Maui benthic habitats using the 'D_STRUCT' class in the attribute table. We retitled the habitat class named 'Rock/boulder' in the 'D_STRUCT' class that

25 corresponded to the descriptor from the 'M_STRUCT' class named 'Coral Reef and Hard Bottom' to clarify that particular substrate type is a coral-dominated habitat. All classes were chosen to provide a common level of benthic habitat detail across study sites. Once the habitat classes were chosen, we exported them as individual shapefiles with ArcMap.

We determined elevation change by habitat using the XYZ_{change} data points. We computed elevation-change statistics from

30 the points included within or on the boundary of each habitat. For a given site, we opened the corresponding XYZ_{change}

shapefile and the polygons defining the boundaries of a given habitat class in ArcMap and applied the 'Select Layer By Location' tool to extract the points falling within or on the boundaries of the habitat. Parameter settings were:

1) set 'Input Feature Layer' to the layer containing the XYZ points;
2) set 'Relationship' to INTERSECT;
3) set 'Selecting Features' to the layer containing the habitat polygons;
4) leave 'Search Distance' blank; and
5) set 'Selection type' to NEW_SELECTION.

We also created an ArcMap 'model' to automate the XYZ_{change} data-point processing for calculation of elevation-change statistics in Table 2, and to ensure consistency for each habitat class. The elevation gain and loss statistics are based on the set of points with elevation changes greater than or less than zero, respectively.

We computed volume changes in accretion and erosion per habitat class using a procedure similar to the one used to compute site-wide changes (see 'Elevation- and volume-change analysis-TIN modeling' section). For a given site and habitat class, we created a new polygon from the intersection of the site-footprint with a habitat-class polygon using the 'Clip' tool. This habitat-extraction polygon was necessary because habitat coverage extended beyond the bounds of each site TIN. With this refined habitat polygon, we applied the 'Edit TIN' tool to the site TIN, creating a new TIN covering only the extent of the specified habitat class. Finally, we performed the same set of surface volume calculations as described in the TIN modeling section. Because these steps had to be repeated for each habitat class for each study site, we created an ArcMap 'model' to automate the process and for calculation of volume-change statistics (Table 3). We determined the amount of elevation and volume change in coral-dominated habitats and adjacent (non-coral dominated) habitats by grouping the elevation and volume change results for the pertinent habitat classes (Tables 2 and 3) and computing combined values for 'coral substrate' and 'adjacent substrate' at each site (Table 1).

2.4 Lower Florida Keys – volume to Pleistocene bedrock

The depth-to-Pleistocene-bedrock (DPB) surface was constructed from seismic data and cores along the Florida Keys reef tract from southern Key Largo through the Dry Tortugas, and was obtained as a shapefile referenced to NAD27 datum at http://pubs.usgs.gov/pp/2007/1751/data/PP1751.zip (Lidz, 2000;Lidz et al., 2007). The difference between a bathymetric surface and DPB surface estimates sediment thickness of the Holocene reef deposit along the Florida Keys reef tract. We clipped the extent of the DPB polygons that corresponded to the extent of the LFK study site using the 2D surface area polygon for the study site and ArcMap 'Analysis tools' > 'Extract' > 'Clip'. Next, we assigned XYZ coordinates to each depth-contour polygon with the assigned Z value equaling the corresponding depth contour using Xtools > 'Table Operations' > 'Add XYZ Coordinates'. We then exported the resulting attribute table as an XYZ-point file to MS Excel

using Xtools > 'Table Operations' > 'Export Table' to MS Excel'. We imported a tab-delimited file format of this XYZ-point file to VDatum, and assigned NAD27 (the published datum) and MLW to the source file, and UTM NAD83 and NAVD88 GEOID03 as the target datums. We reformatted the point file headers in Excel for import to ArcCatalog, created a shapefile, and projected the DPB polygons from NAD27 to UTM NAD83 using 'Data Management Tools' > 'Projections

5 and Transformations' > 'Project'. We then merged the point file with the DPB polygons using 'Analysis Tools' > 'Overlay' > 'Spatial Join' in ArcMap to assign the NAVD88 GEOID03 values from the point file to the polygons. DPB polygons were converted to raster format using 'Conversion Tools' > 'To Raster' > 'Polygon to Raster' tool.

We created a raster DEM for historical bathymetric data for calculation of Holocene reef volume in 1938 using the same

10 Delaunay triangulation algorithm as described in the 'Elevation- and volume-change analysis-TIN Modeling' section with a maximum edge length for triangulation of 900 m and maximum triangle area of 50,000 m. We calculated historical sediment thickness above the Pleistocene bedrock layer using the LFK 1938 DEM by subtracting the DEM surface from the updated DPB layer using 'Spatial Analyst Tools' > 'Map Algebra' > 'Raster Calculator' to create a raster that represented sediment thickness. We compared total Holocene reef volume to recent net volume loss (Table 1) considering that net volume and

15 mass changes from 1938 to 2004 would have converged if reef framework had filled with sediment and accreted rather than eroded. To compute the time required to completely erode the remaining Holocene reef down to the Pleistocene layer, we used a modern reef age of 6000 years (Lidz, 2000) and a constant erosion rate.

2.5 Error analysis

2.5.1 Vertical error analysis

20 U.S. Federal Standards were applied for all vertical and horizontal data transformations and error analyses. To provide conservative estimates of elevation changes, we followed the general approach used by the U.S. Army Corps of Engineers (Byrnes et al., 2002) to compute a composite root-mean-square error (RMSE) for our data (Table 4), according to Eq. (1).

$$RMSE_{Total} = \sqrt{RMSE_{Sounding}^2 + RMSE_{LiDAR}^2 + RMSE_{VDatum}^2} \tag{1}$$

where $RMSE_{Sounding}$ was computed from the historical point data, and $RMSE_{LiDAR}$ was reported in the metadata accompanying the LiDAR data for each site and based on independent validation by in-water acoustic-based depth measurements. Error associated with vertical datum transformation, $RMSE_{VDatum}$, was computed using VDatum version 3.6 (NOAA National Ocean Service, 2016). Note that no vertical transformations were performed for the Maui data because both historical and

30 modern bathymetric data were collected and reported relative to MLLW; therefore, $RMSE_{VDatum}$ was excluded from vertical error estimates for this study site. The maximum cumulative uncertainty (MCU) for operational VDatum regions of South Florida and the Virgin Islands are 9.6 cm and 11.8 cm, respectively (NOAA National Ocean Service, 2016). Our calculated

RMSE$_{VDatum}$ for the Florida Keys, St. Thomas and Buck Island study sites fall within reported MCU values (Table 4).

When historical sounding data were collected, repeat surveys were performed along select transect lines and/or additional soundings were collected along intersecting transects for the purpose of determining vertical accuracy. Only maximum
5   difference of repeat data points was reported as accuracy information in the historical data set descriptive reports. For data collected by the Coast Survey from the late 1800's to 1950's, maximum allowable differences at crossings were 0.06 m for depths less than 4.6 m, and 0.46 m for depths between 22 and 29 m (Byrnes et al., 2002). For data collected from the mid to late 1900's, when positioning and water depth measurements advanced from manual to electronic, maximum allowable water depths at offshore crossings were not to exceed 0.6 m (Byrnes et al., 2002). We used these repeat and cross-track line
10   survey data to perform a more rigorous systematic error analysis of historical depth measurements (Byrnes et al., 2002). For each historical sounding point we computed the distance between it and all the remaining points within a given study site. We retained only those point pairings that were separated by ≤5 m. Given that rapid elevation changes over short distances occur in coral reef environments, we further filtered the pairs, keeping those with an absolute depth difference of ≤ 0.5 m, i.e., $\left| d_{i,1} - d_{i,2} \right| \leq 0.5$, where $d_{i,1}$ and $d_{i,2}$ are the depths of the two points in the i-th pair. Applying this threshold avoids
15   sharp drop-offs, such as channel edges and situations were one point is on the reef and the adjacent point is in a depression or off the reef. We set the threshold at 0.5 m because it was greater than both the measurement resolution for any data set and the largest measurement difference between reported replicate values for those data sets that reported replicates. With the remaining paired points, we computed $RMSE_{Sounding}$ according to Eq. (2) for n point pairings.

$$RMSE_{Sounding} = \sqrt{\frac{\sum_{i=1}^{n}\left(d_{i,1} - d_{i,2}\right)^2}{n}}$$

(2)

The number of sounding points pairs used for each location was 40, 253, 40, and 51 for the UFK, STT, STC and Maui, respectively. The LFK was excluded from this analysis because no adjacent points were separated by 5 m or less. Implicit in this approach is the assumption that the points in each pairing represent two independent depth measurements at
25   approximately the same location. Therefore, the mean difference in depth between all pairs should not be significantly different from 0 m. For each study site, we performed a 2-tailed t-test at the $\alpha = 0.05$ level on the set of depth differences between paired points to test the null hypothesis of a zero mean difference. All of the RMSE calculations and t-tests were performed using Matlab v8.4.0 (R2014b), and are reported in Table 4.

30   Using the individual RMSE$_{Total}$ values, we computed a single, more conservative RMSE value that was applied to all five study sites. We considered the RMSE$_{Total}$ values from each study site to be proxies for the standard deviations (σ). In a

normal distribution, 1-σ encompasses approximately 68% of the variability and 2-σ encompasses approximately 95%. We chose to multiply the RMSE$_{Total}$ values by 1.65, capturing approximately 90% of the variability in the depth differences. The average of these new values was 0.48 m, which we rounded to 0.5 m and applied as a global RMSE applicable to all of our study sites to compute the minimum bound of the volume change estimates. Our average RMSE$_{Total}$ (0.29 m) is similar to

5 that reported for lidar and acoustic sounding data and half the reported value for previous studies that used nautical chart data to create a digital elevation model for examining the response of a reef to sea level rise (Leon, 2013b;Hamylton, 2014).

2.5.2 Horizontal error analysis

All horizontal datums of the historical XYZ data were converted to North American Datum 1983 (NAD83) by NOAA during the digitization of historical smooth sheets. No horizontal error was reported for any historical data sets. Our

10 historical sounding data ranged from the 1930's to 1980's. Visual inspections of georectified historical H-sheets overlain on modern georectified aerial imagery of 1 m resolution showed good alignment between coastal and geographic features (2016 World Imagery from ArcGIS online via ArcMap 10.2.2, source: Esri, DigitalGlobe, GeoEye, Earthstar Geographics, CNES/Airbus DS, USDA, USGS, AEX, Getmapping, Aerogrid, IGN, IGP, swisstopo, and the GIS User Community). We determined the potential horizontal error associated with our oldest data sets from the 1930's (Florida Keys), measured using

15 triangulation methods, and used this as an estimate of maximum horizontal error for all study sites.

The original horizontal datum for data sets from the Florida Keys was North American Datum 1927 (NAD27). Conversion of data from NAD27 to NAD83 using NOAA National Ocean Service program NADCON introduces no more that 15 cm of uncertainty in the continental United States (Dewhurst, 1990). The Annual Report of the U.S. Coast and Geodetic Survey

20 192 (1880) indicates that it was possible under normal controls to measure distances (using triangulation) with an accuracy of 1 meter, and the position of the plane table could be determined within 2 to 3 meters of its true position (Shalowitz, 1964). The horizontal resolution of LiDAR data is reported as better than 1m (Brock et al., 2006; Brock et al., 2007; Fredericks et al., 2015a, b). A sum of estimated sources of error is, therefore, approximately 5 m (maximum uncertainty from NADCON conversion + accuracy of triangulated distance measurements + accuracy of plane table position + horizontal resolution of

25 LiDAR data). During visual inspection of H-sheets, we measured, for example, a maximum difference of 4.8 m between the position of a historical bridge structure located south of Lower Matecumbe Key in the UFK as depicted on a 1934 H-sheet and on the 2016 World Imagery. This offset is consistent with the sum of estimated horizontal uncertainties that include historical position measurements using triangulation.

30 We minimized horizontal uncertainties due to data density and track line orientation by extracting modern data points from high-resolution LiDAR DEMs (1 to 4 m) at the location of the more coarsely distributed historical data points. We created a single TIN model from the calculated elevation differences (Z$_{change}$) between these points for volume change analyses, rather

than determining volume change by comparing separate historical and modern TIN models. We performed a horizontal shift analysis to test the potential impact for systematic plus random horizontal error of up to 10 m. We chose 10 m as a conservative value because it represents an approximate doubling of the sum of estimated sources of error (5.0 m), as well as a doubling of the maximum observed offset of a fixed structure in our data set (4.8 x 2 = 9.6 m). Historical XYZ elevation

5   data from the Upper and Lower Florida Keys were shifted by 10 meters to the north, south, east and west by adding 10 m to, and subtracting 10 m from, UTM northings and eastings for each data point (26,341 and 1,688 points for the Upper and Lower Florida Keys, respectively). This exercise generated 4 new, experimental historical XYZ point-data sets that simulate up to 10 meters of horizontal error in each of 4 directions. We used these experimental data sets to create new shapefiles for each study site. Un-shifted LiDAR DEMs were clipped to each shifted historical shapefile, then corresponding elevations

10   from the LiDAR DEMs were extracted at each historical point location and used to calculate elevation differences between the shifted historical soundings and un-shifted LiDAR data sets as previously described. We created new TIN models from the shifted XYZ point-data sets and calculated volume changes for each of these data sets using the TIN modeling process and surface volume analysis previously described (this study).

15   Results from the horizontal shift analysis indicate that 10 m of horizontal error produces no more than 10% difference in net and area-normalized volume change calculations in the Upper Florida Keys, and up to a 21% difference in the Lower Florida Keys (likely due to a lower density of data points over a smaller geographic area). Imparting 10 m of error in these experimental data sets does not change the general conclusion of our study indicating high magnitude of net erosion at these study sites. Our results are consistent with reports that over large areas (such as in our study), random errors largely cancel-

20   out relative to change calculations derived from two surfaces (Byrnes et al., 2002).

3 Results

3.1 Regional-scale loss of mean seafloor elevation and volume

Loss of seafloor elevation and volume, and transition from net accretion to net erosion, has occurred at all study sites (Table 1). Mean seafloor elevation losses ranged from -0.09 m to -0.8 m across all of these regions. These regional mean values

25   ('Mean elevation-change' column in Table 1) represent the net change encompassing all positive (elevation-gains) and negative (elevation-losses) values. Large ranges of elevation change were observed within each study site with maximum losses exceeding 4.0 m and maximum gains exceeding 6.5 m resulting in high standard deviations of 0.7 m to 1.5 m for all sites (Table 2).

30   Examination of only those locations within habitats where elevation-losses occurred ('Mean loss' column in Table 2) indicates that, of the 59 individual habitat analyses we performed across all five study sites, only two habitats showed mean losses less than our $RMSE_{Total}$ of 0.29. Only 14 habitats showed mean losses less than our 1.65 x $RMSE_{Total}$ of 0. 5 m (that

encompasses 90% of the variability). Therefore, mean losses in 97% of the habitats we analyzed were greater than our vertical $RMSE_{Total}$ of 0.29 m, and 77% of the habitats we analyzed showed mean losses greater than 1.65 x $RMSE_{Total}$ of 0.5 m. In several cases, and particularly associated with coral-dominated substrate, mean losses exceeded 1 meter ('Mean loss' column in Table 2). Conversely, examination of only those locations within habitats where elevation gains occurred ('Mean

5 gain' column in Table 2) indicates that 92% of the 59 habitats showed mean elevation-gains greater than our $RMSE_{Total}$, and 60% showed mean gains greater than our 1.65 x $RMSE_{Total}$.

Net volume losses were also observed in all regions indicating export of sediments from these systems (Table 1). Minimum volume changes (calculated by excluding elevation change data within a vertical range of ±0.5 m, see 1.65 x RMSE

10 calculations in Table 4) provide conservative estimates of net volume losses ranging from 0.2 to 52.8 million cubic meters (Mm^3). Maximum volume changes (including all elevation-change data) indicate net volume losses ranging from 3.4 to 80.5 Mm^3 for all study sites. We did not convert volume to mass of calcium carbonate because volume change includes sediment compaction, loss due to mortality and degradation of framework-building coral colonies, and sediments of various porosities.

3.2 Changes in mean seafloor elevation and volume by habitat type

15 Mean elevation and volume losses occurred in 78% of the 59 individual habitats that we examined (Table 2). Greatest mean elevation losses were generally associated with shallow, coral-dominated habitats (Table 1 and Table 2) at all study sites consistent with observations of general flattening (Alvarez-Filip et al., 2009) of reef topography and observations of decreasing abundance of reef-building corals (Gardner et al., 2003; Bruno and Selig, 2007; 2014). However, greatest net volume losses were generally associated with adjacent (non-coral dominated) habitats despite smaller mean elevation losses

20 due to their greater areal extent (Table 1 and Table 3). Maximum values of area-normalized volume change calculated using all elevation change data (Table 1) indicate that volume loss in adjacent habitats was 40% to 100% of losses observed in coral-dominated substrate. Areal extent of coral-dominated substrate was only 8% to 15% of the total study area in the Upper and Lower Florida Keys and St. Thomas, and contributes up to only 26% of the total net volume loss. Areal extent of coral-dominated substrate was much higher at the Maui study site, 57%, and contributed more than 50% to net volume loss. The

25 considerable loss of seafloor volume in adjacent habitats at these study sites and large total net volume losses suggests that physical erosion of adjacent habitats and export of sediments is a likely driver of much of the volume loss we observed at these study sites rather than degradation of high porosity, large framework-building corals and redistribution of sediments within the system. Buck Island showed the lowest net volume and mean elevation loss, and the highest areal extent of coral-dominated substrate (91%) that contributed more than 90% to net volume loss, suggesting that degradation of framework-

30 building corals may be the primary contributor to volume loss at this study site and much less sediment has been exported.

Along the Florida Keys reef tract within Biscayne National Park, Florida and the Florida Keys National Marine Sanctuary, mean elevation and volume losses occurred in 9 of 11 habitat classes in the Upper Florida Keys (UFK) reef tract (Fig. 1a, b)

and in 6 of 9 classes in the Lower Florida Keys (LFK) reef tract (Fig. 1c, d) including coral habitats, and adjacent habitats such as unconsolidated sediments, pavement previously covered by sediments or coral, and seagrass. Largest mean elevation losses occurred at shallow patch and aggregate reefs, coral-dominated and reef rubble habitats, consistent with documented declines in abundance of large framework-building corals over the past several decades (2014). Largest net volume losses occurred in seagrass and unconsolidated sediment habitats. Mean elevation and volume gains occurred in deep water habitats including offshore aggregate reefs in the LFK near a sanctuary preserve area, at the base of spur-and-groove habitat along fore-reef slopes, and where relic spur-and-groove formations in-filled with sediments indicating transport of reef sediments down the fore-reef slope and export offshore. Mean total elevation loss was lowest at the UFK study site. However, mean elevation losses decreased from upper (-0.4 m) to central (-0.3 m) sub-regions of the UFK, and mean elevation increased slightly in the lower sub-region (0.1 m) primarily associated with seagrass habitat (Fig. 1a, b). Notably, the lower sub-region is further away from high-density population areas north of the study site and near an area of the middle Florida Keys identified as a possible refuge from ocean acidification due to seagrass productivity (Manzello et al., 2012). The LFK site included the Looe Key National Marine Sanctuary and Special Protection Area (Fig. 1c). Net elevation and volume losses were similar to the central sub-region of the UFK possibly due to close proximity to high-density population areas in the Lower Florida Keys. However, the LFK was the only study site that showed net accretion in combined coral habitat classes. Accretion is partially attributed to deep reef and spur-and-groove habitat that has been buried by sand (Lidz et al., 2007). Redistribution of reef materials and erosion of the Florida reef tract is corroborated by field observations of movement and deposition of meters-thick sand deposits likely due to hurricanes and by exposure of older reef material from erosion and transport (Shinn et al., 2003). However, accretion was also observed on offshore aggregate reef habitat near the Special Protection Area.

Mean elevation and volume loss occurred in 16 of 17 habitat classes in St. Thomas, USVI (STT, Fig. 2a, b). However, uninhabited Buck Island National Reef Monument and Marine Park, St. Croix USVI (BI) showed less mean elevation and volume loss than all other sites with losses limited to 4 of 11 habitat classes including 3 coral habitats (Fig. 2c, d). In STT, small, localized areas of coral-dominated substrate showed gains in elevation. However, greatest mean elevation losses occurred in coral-dominated habitats and near the central coastline where harbor and shipping channels exist. Mean elevation and volume gains only occurred on un-colonized bedrock possibly due to transport and deposition of sediments. The study period for BI is approximately 10 years shorter than for nearby STT. Greatest mean elevation gains in BI occurred along linear reef near the shoreline. Most elevation and volume gains occurred within Buck Island National Reef Monument and Marine Park boundaries (Fig. 2c) suggesting that distance from populated areas combined with managed protection has limited losses at this site.

Mean elevation and volume loss occurred in 10 of 12 classes in Maui (Fig. 3a, b). Mean elevation and area-normalized volume losses were at least 2 to 3 times greater, respectively, than all other study sites and occurred over a shorter time-

frame. These greater losses may be caused by higher sediment export rates due to a combination of higher wave energy, physical erosion and a narrow shallow shelf surrounding the island allowing sediment to be more easily transported offshore into deep water, as has been observed in other high energy reef environments (Morgan, 2014; Perry, 2015). Greatest mean elevation losses were associated with coral-dominated habitat as well as 'not classified' habitat located in the bank/shelf

5   zone that may be impacted by slumping of materials along steeply sloping areas. Elevation and volume gains occurred in mud and rubble habitats, and may be associated with terrigenous sediment transport from the island.

4 Discussion

Our results include elevation and volume changes caused by chronic erosion processes that occur slowly over time frames of months to decades such as changes in carbonate production rates, bioerosion, chemical erosion from carbonate dissolution,

10   degradation of large framework building coral colonies, and physical movement of reef sediments due to persistent oceanographic conditions such as waves and currents. Our results also include changes caused by episodic events that occur over very short time frames of minutes to days, and often cause large changes in elevation. Examples include dredging and infilling of channels and coastal harbors, deposition of terrigenous materials from landslides and run-off, slumping and relocation of seafloor materials at steeply sloping locations, storm erosion and deposits. We included large elevation-change

15   data in our calculations likely caused from these episodic events because such changes affect process modeling for hazards analysis and alter habitat distribution. We note that much reef degradation contributing to elevation change likely occurred after 1970 (Gardner et al., 2003; Bruno and Selig, 2007; 2014). Therefore, data sets containing pre-1970's data (Table S1) could be biased toward lower annual elevation and volume-change rates.

20   Over 90% of the habitats we analyzed in our study showed statistically significant elevation-changes with a net result of elevation loss. Erosion of both coral-dominated substrate and non-coral substrate suggests that the current rate of carbonate production is no longer sufficient to support net accretion of coral reefs or adjacent habitats. Our results indicate that mean seafloor elevation decreased by -1.5 to -6.3 mm yr^{-1} over 33 to 68 years at Atlantic and Caribbean sites, and by -21.1 mm yr^{-1} over 38 years at the Pacific site (Fig. 4). These elevation changes are equivalent to loss of 34 to 115 years of reef accretion

25   based on average Holocene reef accretion rates of 2.6 and 10 mm yr^{-1} for Caribbean/Atlantic and Pacific reefs, respectively (Shinn et al., 1977; Buddemeier and Smith, 1988). Coral reefs in all three regions have lost pace with historical global mean sea level rise of 1.7 mm yr^{-1} between 1901 and 2010, and will be unable to keep up or catch up with current or projected rates of 3.2 mm yr^{-1} (1993-2012) and 4.5 mm yr^{-1} (mid-century, RCP4.5), respectively (Church et al., 2013).

30   The seafloor elevation and volume losses observed in our study indicate the extent of erosion that has already occurred in many coral reef ecosystems may be largely under-estimated without comprehensive analysis of total elevation and volume change. Without such analyses, assessments of risk levels and impact from coastal hazards due to coral reef degradation may

also be under-estimated. Recent estimates of modern reef accretion and erosion rates on Caribbean reefs based on only carbonate production and bioerosion indicate average potential accretion of 1.36 mm yr^{-1} and range from -1.17 to 11.93 mm yr^{-1} (Perry et al., 2013). Assuming a maximum erosion rate of -1.17 mm yr^{-1} (Perry et al., 2013), reduced carbonate production and bioerosion could account for as much as 65% of the erosion we observed at Buck Island (-1.8 mm yr^{-1}), but

5 only 19% of erosion observed at St. Thomas (-6.3 mm yr^{-1}). Recent regional-scale measurements of carbonate production and dissolution in the Florida Reef Tract show that dissolution alone could account for chemical erosion of up to approximately -0.7 mm yr^{-1} in the northernmost reef tract (Muehllehner, 2016), or approximately 12% of the erosion we observed in the upper region of the Upper Florida Keys (-0.4 m total or -5.9 mm yr^{-1}). Combining maximum estimates for reduced carbonate production, bioerosion and chemical dissolution could account for much of the elevation loss at BI, but

10 only approximately 30% of erosion at STT and the UFK. Our results indicate that as much as 35 to 88% of erosion in these regions may be attributed to physical processes and/or export of reef sediments from these systems that has been unaccounted for in previous assessments of seafloor accretion and erosion rates in modern coral reef ecosystems. These values are similar to sediment export estimates ranging from 20% to greater than 50% on a Maldivian reef platform along sheltered and exposed reef margins, respectively (Morgan, 2014; Perry, 2015).

The magnitude of regional-scale erosion, millions of cubic meters, from these reef systems (Table 1) following world-wide declines and transitions in reef species composition combined with projections for continued global reef degradation suggests the onset in the geologic record of an Anthropocene reef crisis (Kiessling and Simpson, 2011). For example, we calculated that Holocene reef volume at the LFK site was 101.2 Mm^3 in 1938 by performing a difference analysis between

20 the 1938 historical DEM (this study) and a georectified map of depth-to-Pleistocene bedrock (Lidz, 2000). Comparison of total Holocene reef volume in 1938 to net volume loss from 1938 to 2004 (Table 1) indicates that Holocene reef volume has decreased by as much as 5% over the past 66 years and that the reef is eroding 5 times faster than it accreted throughout the Holocene. Assuming a modern reef age of 6000 years (Lidz, 2000) and a constant erosion rate, total reef volume at this location could completely erode down to Pleistocene-bedrock-surface in approximately 1250 years.

Previous studies indicate that, in some cases, higher sea level will facilitate production and transport of unconsolidated sediments shoreward, and growth of reef islands (Hopley, 1988; Hopley, 1992). However, our results indicate net export of sediments from the regions in our study as well as evidence for offshore transport of materials. Studies of ancient reefs indicate that many were able to keep up or catch up with sea level rise (Neumann A.C., 1985). However, ancient reefs that

30 were exposed to local, regional and global environmental stresses were unable to keep up and drowned (Schlager, 1981; Hubbard, 1997; Kiessling and Simpson, 2011). Recent projections of reef response to sea level rise in the northern Great Barrier Reef using carbonate production rates primarily from the 1970's indicate that shallower reef flats could become colonized by corals with a rise in sea level of 0.5 m, but begin to drown after 30 years with a rise of 1.2 m (Hamylton, 2014). However, these projections do not consider reduced rates of calcification due to local and global stressors and loss of

carbonates from erosion processes. Chagos Archipelago reef systems in the Indian Ocean that are both geographically isolated and lack human impacts show high accretion rates and the ability to recover from bleaching events (Perry, 2015). However, the large erosion rates we observed in Maui suggest that heavily populated islands may not recover despite geographic isolation. We observed lower erosion rates in reef ecosystems that were managed, distant from human population

5 centers, or associated with natural refuge zones; however, these lower rates did not prevent net regional-scale losses of seafloor elevation and volume. Modern carbonate production rates are an order of magnitude lower than Holocene averages (Perry et al., 2013), and are estimated to decrease by as much as 60% by mid-century (Langdon and Atkinson, 2005). Bioerosion and chemical dissolution of carbonates will increase with ocean acidification (Hoegh-Guldberg et al., 2007; Eyre et al., 2014; Enochs, 2015). Therefore, reef erosion rates are likely to accelerate over the coming decades.

Numerical models indicate that loss of reef structure and seafloor elevation increases coastal vulnerability to erosion, storm surge, waves, sea level rise and tsunami hazards that are predicted to intensify and become more frequent with global climate change (Lowe et al., 2005; Quataert et al., 2015). An increase in water depth of 0.5 to 1.0 m from rising sea level by 2100 is projected to cause larger waves and accelerated physical erosion of sediments on fringing reef flats and adjacent coastlines

15 (Storlazzi et al., 2011). Our results show that degradation of coral reef ecosystems in Atlantic, Caribbean and Pacific regions has accelerated the relative increase in water depth from sea level rise, and has already increased water depths to levels that were not expected until near 2100. We projected increases in water depth at our study sites based on our measured rates of mean elevation loss combined with sea level rise. Our projections indicate that seafloor erosion will increase water depths by 2 to 8 times more than levels predicted from sea level rise alone by the year 2100 at all study sites (Fig. 5, Table S9). The

20 divergence between rising sea level and declining seafloor elevation has already increased the risk to coastlines in these regions from long-term, persistent oceanographic pressures and periodic events such as storms. The combination of human impacts to reefs and unprecedented rates of global climate change are likely to intensify coastal hazard vulnerabilities caused by seafloor erosion in coral reef ecosystems over the next century.

Author contributions

25 K.K. Yates and D.G. Zawada conceived of and designed the research project, interpreted the results, and wrote the manuscript. N.A. Smiley acquired and processed the historical data sets. G. Tiling-Range created the ArcGIS models to automate computation of the habitat-related statistics.

Acknowledgements

We thank N. Buster for assistance with preparation of historical data for geospatial analysis and review of methods sections,
30 and X. Fredericks for assistance with development of LiDAR digital elevation models. N. Plant provided advice and

comments on elevation surface modeling and error propagation statistics. We thank C. Moore for help with manuscript formatting. M. Michalski, J. Campagnoli, M. Cole, S. White, T. Ehret provided assistance with and information for validation of metadata for historical bathymetry data from NOAA. N. Johnston provided assistance with LiDAR data access and metadata from the Joint Airborne Lidar Bathymetry Center of Expertise (JALBTCX). This work was supported and

5 funded by the U.S. Geological Survey - Coastal and Marine Geology Program. Use of trade, firm or product names is for descriptive purposes only and does not imply endorsement by the U.S. Government.

References

Alvarez-Filip, L., Dulvy, N. K., Gill, J. A., Cote, I. M., and Watkinson, A. R.: Flattening of Caribbean coral reefs: Region-wide declines in architectural complexity, Proc. R. Soc. Biol. Sci. Ser. B, 276, 3019-3025, doi:10.1098/rspb.2009.0339,

10 2009.

Aronson, R. B., Macintyre, I. G., Precht, W. F., Murdoch, T. J. T., and Wapnick, C. M.: The expanding scale of species turnover events on coral reefs in Belize, Ecol. Monogr., 72, 233-249, 2002.

Battista, T. A., and Christensen, J.: Benthic habitat mapping of main Hawaiian Islands, NOAA National Centers for Coastal Ocean Science, Biogeography Branch, Silver Spring, MD,

15 http://products.coastalscience.noaa.gov/collections/benthic/e97hawaii/data2007.aspx, 2007.

Brock, J. C., Wright, C. W., Patterson, M., Nayegandhi, A., Patterson, J., Harris, M. S., and Mosher, L.: EAARL submarine topography—Biscayne National Park, U.S. Geological Survey, USGS Open-File Report 2006-1118, http://pubs.usgs.gov/of/2006/1118/, last access: 22 Sept. 2016, 2006.

Brock, J. C., Wright, C. W., Nayegandhi, A., Patterson, M., Travers, L. J., and Wilson, I.: EAARL submarine topography -

20 Northern Florida Keys Reef Tract, U.S. Geological Survey, USGS Open-File Report 2007-1432, http://pubs.er.usgs.gov/publication/ofr20071432, last access: 22 Sept. 2016, 2007.

Brock, J. C., Yates, K.K., Halley, R.B., Kuffner, I.B., Wayne Wright, C., Hatcher, B.G.: Northern Florida Reef Tract benthic metabolism scaled by remote sensing, Mar. Ecol. Prog. Ser., 312, 123-139, 2006.

Bruno, J. F., and Selig, E. R.: Regional decline of coral cover in the Indo-Pacific: Timing, extent, and subregional

25 comparisons, PLoS One, 2, doi:10.1371/journal.pone.0000711, 2007.

Buddemeier, R. W., and Smith, S. V.: Coral-reef growth in an era of rapidly rising sea-level - predictions and suggestions for long-term research, Coral Reefs, 7, 51-56, doi:10.1007/bf00301982, 1988.

Burke, L., Reytar, K., Spalding, M., and Perry, A.: Reefs at risk revisited, World Resources Institute, Washington D.C., 130 pp., 2011.

30 Buster, N. A., and Morton, R. A.: Historical bathymetry and bathymetric change in the Mississippi-Alabama coastal region, 1847–2009, Scientific Investigations Map 3154, U.S. Geological Survey, USA, http://pubs.usgs.gov/sim/3154/, 2011.

Byrnes, M. R., Baker, J. L., and Li, F.: Quantifying potential measurement errors and uncertainties associated with bathymetric change analysis, Vicksburg, MS, ERDC/CHL CHETN-IV-50, 17 pp., 2002.

Byrnes, M. R., Rosati, J. D., Griffee, S. F., and Berlinghoff, J. L.: Historical sediment transport pathways and quantities for determining an operational sediment budget: Mississippi Sound Barrier Islands, J. Coast. Res., 166-183, doi:10.2112/si63-

5   014.1, 2013.

Church, J. A., Clark, P. U., Cazenave, A., Gregory, J. M., Jevrejeva, S., Levermann, A., Merrifield, M. A., Milne, G. A., Nerem, R. S., Nunn, P. D., Payne, A. J., (UK), W. T. P., Stammer, D., and Unnikrishnan, A. S.: Sea level change, in: Climate Change 2013: The Physical Science Basis. Contribution of Working Group I to the Fifth Assessment Report of the Intergovernmental Panel on Climate Change, edited by: Stocker, T. F., Qin, D., Plattner, G.-K., Tignor, M., Allen, S. K.,

10   Boschung, J., Nauels, A., Xia, Y., Bex, V., and Midgley, P. M., Cambridge University Press, Cambridge, New York, 1137–1216, 2013.

Dewhurst, W. T.: NADCON: The application of minimum-curvature-derived surfaces in the transformation of positional data from the North American Datum of 1927 to the North American Datum of 1983, NOAA Technical Memorandum, NGS-50, 32 pp., 1990.

15   Enochs, I. C., Manzello, D.P., Carton, R.D., Graham, D.M., Ruzicka, R, and Collela, M.A.: Ocean acidification enhances the bioerosion of a common coral reef sponge: Implications for the persistence of the Florida Reef Tract, Bull. Mar. Sci., 91, 271-290, doi:10.5343/bums.2014.1045, 2015.

Eyre, B. D., Andersson, A. J., and Cyronak, T.: Benthic coral reef calcium carbonate dissolution in an acidifying ocean, Nat. Clim. Change, 4, 969-976, doi:10.1038/nclimate2380, 2014.

20   Ferrario, F., Beck, M. W., Storlazzi, C. D., Micheli, F., Shepard, C. C., and Airoldi, L.: The effectiveness of coral reefs for coastal hazard risk reduction and adaptation, Nat. Comm., 5, doi:10.1038/ncomms4794, 2014.

Florida Fish and Wildlife Conservation Commission: The Unified Florida Reef Tract map, Florida Fish and Wildlife Conservation Commission, http://ocean.floridamarine.org/IntegratedReefMap/UnifiedReefTract.htm, last access: 22 Sept. 2016, 2015.

25   Fredericks, X., Kranenburg, C. J., and Nagle, D. B.: EAARL-B submerged topography—Saint Croix, U.S. Virgin Islands, 2014, U.S. Geological Survey, USGS Data Release, http://coastal.er.usgs.gov/data-release/doi-F73T9F86/, last access: 22 Sept. 2016, 2015a.

Fredericks, X., Kranenburg, C. J., and Nagle, D. B.: EAARL-B submerged topography—Saint Thomas, U.S. Virgin Islands, 2014, U.S. Geological Survey, USGS Data Release, http://coastal.er.usgs.gov/data-release/doi-F7G15XXG/, last access: 22

30   Sept. 2016, 2015b.

Frieler, K., Meinshausen, M., Golly, A., Mengel, M., Lebek, K., Donner, S. D., and Hoegh-Guldberg, O.: Limiting global warming to 2 degrees C is unlikely to save most coral reefs, Nat. Clim. Change, 3, 165-170, doi:10.1038/nclimate1674, 2013.

Garcia, S. M., and Moreno, I. d. L.: Global overview of marine fisheries, in: Responsible Fisheries in the Marine Ecosystem, edited by: Sinclair, M., and Valdimarsson, G., Centre for Agriculture and Biosciences International (CABI), 448, 2003.

Gardner, T. A., Cote, I. M., Gill, J. A., Grant, A., and Watkinson, A. R.: Long-term region-wide declines in Caribbean corals, Science, 301, 958-960, doi:10.1126/science.1086050, 2003.

5 Glynn, P. W.: Widespread coral mortality and the 1982-83 El Niño warming event, Environ. Conserv., 11, 133-146, 1984.

Greenstein, B. J., Curran, H. A., and Pandolfi, J. M.: Shifting ecological baselines and the demise of *Acropora cervicornis* in the western North Atlantic and Caribbean Province: A Pleistocene perspective, Coral Reefs, 17, 249-261, doi:10.1007/s003380050125, 1998.

Hamylton, S. M., Leon, J.X., Saunders, M.I. and Woodroffe, C.D.: Simulating reef response to sea-level rise at Lizard

10 Island: A geospatial approach, Geomorphology, 222, 151-161, 2014.

Hoegh-Guldberg, O., Mumby, P. J., Hooten, A. J., Steneck, R. S., Greenfield, P., Gomez, E., Harvell, C. D., Sale, P. F., Edwards, A. J., Caldeira, K., Knowlton, N., Eakin, C. M., Iglesias-Prieto, R., Muthiga, N., Bradbury, R. H., Dubi, A., and Hatziolos, M. E.: Coral reefs under rapid climate change and ocean acidification, Science, 318, 1737-1742, doi:10.1126/science.1152509, 2007.

15 Hopley, D.: Coral reefs in a period of global sea level rise, in: Recent Advances in Marine Science and Technology 1992, edited by: Saxena, N. K., PACON, Honolulu, 453-462, 1992.

Hopley, D. a. K., D.W.: The effects of rapid short term sea level rise on the Great Barrier Reef, in: Greenhouse Planning for Climate Change, edited by: Pearman, G. I., Brill, Leiden, 189-201, 1988.

Hubbard, D. K.: Reefs as dynamic systems, in: Life and Death of Coral Reefs, edited by: Birkeland, C., Chapman & Hall,

20 New York, 43-67, 1997.

Jackson, J., Donovan, M., Cramer, K., and Lam, V. (Eds.): Status and trends of Caribbean coral reefs: 1970-2012, Global Coral Reef Monitoring Network, IUCN, Gland, Switzerland, http://cmsdata.iucn.org/downloads/caribbean_coral_reefs___status_report_1970_2012.pdf, last access: 22 Sept. 2016, 306 pp., 2014.

25 Kench, P. S., and Mclean, R.F.: Hydrodynamics and sediment flux of HOA in an Indian Ocean atoll, Earth Surface Processes and Landforms, 29, 933-953, doi:10.1002/esp.1072, 2004.

Kennedy, Emma V., Perry, Chris T., Halloran, Paul R., Iglesias-Prieto, R., Schönberg, Christine H. L., Wisshak, M., Form, Armin U., Carricart-Ganivet, Juan P., Fine, M., Eakin, C. M., and Mumby, Peter J.: Avoiding coral reef functional collapse requires local and global action, Curr. Biol., 23, 912-918, 2013.

30 Kiessling, W., and Simpson, C.: On the potential for ocean acidification to be a general cause of ancient reef crises, Global Change Biol., 17, 56-67, doi:10.1111/j.1365-2486.2010.02204.x, 2011.

Langdon, C., and Atkinson, M. J.: Effect of elevated pCO(2) on photosynthesis and calcification of corals and interactions with seasonal change in temperature/irradiance and nutrient enrichment, J. Geophys. Res., Oceans, 110, doi:10.1029/2004jc002576, 2005.

Leon, J. X., & Woodroffe, C.D.: Morphological characterisation of reef types in Torres Strait and an assessment of their carbonate productions, Mar. Geol., 338, 64-75, 2013a.

Leon, J. X., Phinn, S.R., Hamylton, S., and Saunders, M.I.: Filling the 'white ribbon' - a multisource seamless digital elevation model for Lizard Island, northern Great Barrier Reef, Int. J. Remote Sens., 34, 6337-6354, 2013b.

5   Lidz, B. H.: Bedrock beneath reefs: The importance of geology in understanding biological decline in a modern ecosystem, U.S. Geological Survey, USGS Open File Report 00-046, http://pubs.usgs.gov/of/2000/of00-046/, last access: 22 Sept. 2016, 2000.

Lidz, B. H., Reich, C. D., and Shinn, E. A.: Systematic mapping of bedrock and habitats along the Florida Reef Tract— Central Key Largo to Halfmoon Shoal (Gulf of Mexico), U.S. Geological Survey, USGS Professional Paper 1751,

10   http://pubs.usgs.gov/pp/2007/1751/, last access: 22 Sept. 2016, 2007.

Lowe, R. J., Falter, J. L., Bandet, M. D., Pawlak, G., Atkinson, M. J., Monismith, S. G., and Koseff, J. R.: Spectral wave dissipation over a barrier reef, J. Geophys. Res., Oceans, 110, doi:10.1029/2004jc002711, 2005.

Madin, J. S., and Madin, E. M. P.: The full extent of the global coral reef crisis, Conserv. Biol., doi:10.1111/cobi.12564, 2015.

15   Manzello, D. P., Enochs, I. C., Melo, N., Gledhill, D. K., and Johns, E. M.: Ocean acidification refugia of the Florida Reef Tract, PLoS One, 7, doi:10.1371/journal.pone.0041715, 2012.

Morgan, K. M. a. K., P.S.: A detrital sediment budget of a Maldivian reef platform, Geomorphology, 222, 122-131, 2014.

Moses, C. S., Andrefouet, S., Kranenburg, C.J., & Muller-Karger, F.E.: Regional estimates of reef carbonate dynamics and productivity using Landsat 7 ETM+, and potential impacts from ocean acidification, Mar. Ecol. Prog. Ser., 380, 103, 2009.

20   Muehllehner, N., Langdon, C., Venti, A., and Kadko, D.: Dynamics of carbonate chemistry, production and calcification of the Florida Reef Tract (2009-2010): Evidence for seasonal dissolution, Global Biochemical Cycles, 30, 661-688, doi:10.1002/2015GB005327, 2016.

Neumann A.C., M., I.: Reef response to sea level rise: keep-up, catch-up, or give-up, Fifth International Coral Reef Congress, Tahiti, 1985, 105-118, 1985.

25   NOAA National Ocean Service: Estimation of Vertical Uncertainties in VDatum, NOAA, http://vdatum.noaa.gov/docs/est_uncertainties.html, last access: 22 Sept. 2016, 2016.

Hydrographic Survey Database Query: http://www.ngdc.noaa.gov/nndc/struts/form?t=103118&s=1&d=1&d=2, last access: 22 Sept. 2016.

Pandolfi, J. M., Bradbury, R. H., Sala, E., Hughes, T. P., Bjorndal, K. A., Cooke, R. G., McArdle, D., McClenachan, L.,

30   Newman, M. J. H., Paredes, G., Warner, R. R., and Jackson, J. B. C.: Global trajectories of the long-term decline of coral reef ecosystems, Science, 301, doi:955-958, doi:10.1126/science.1085706, 2003.

Parker, B. B.: Sea level as an indicator of climate and global change, Mar. Technol. Soc. J., 25, 1992.

Perry, C. T., Murphy, G. N., Kench, P. S., Smithers, S. G., Edinger, E. N., Steneck, R. S., and Mumby, P. J.: Caribbean-wide decline in carbonate production threatens coral reef growth, Nat. Comm., 4, doi:10.1038/ncomms2409, 2013.

Perry, C. T., Murhy, G. N., Kench, P. S., Edinger, E. N., Smithers, S. G., Steneck, R. S., and Mumby, P. J.: Changing dynamics of Caribbean reef carbonate budgets: emergence of reef bioeroders as critical controls on present and future reef growth potential, Proc. R. Soc. Biol. Sci. Ser. B, 281, doi:10.1098/rspb.2014.2018, 2014.

Perry, C. T., Murphy, G.N., Nicholas, A.J., Graham, Wilson, S.K., Januchowski-Hartly, F.A., and East, H.K.: Remote coral

5   reefs can sustain high growth potential and may match future sea-level trends, Scientific Reports, 5, doi:10.1038/srep18289, 2015.

Quataert, E., Storlazzi, C., van Rooijen, A., Cheriton, O., and van Dongeren, A.: The influence of coral reefs and climate change on wave-driven flooding of tropical coastlines, Geophys. Res. Lett., 42, 6407-6415, doi:10.1002/2015gl064861, 2015.

10   Benthic Habitat Maps of the U.S. Virgin Islands-St. Croix prepared by visual interpretation from remote sensing imagery collected by NOAA, 1999: http://catalog.data.gov/dataset/benthic-habitat-maps-of-the-u-s-virgin-islands-st-croix-prepared-by-visual-interpretation-1999c2ef9, last access: 22 Sept. 2016, 2001a.

Benthic Habitat Maps of the U.S. Virgin Islands-St. Thomas and St. John prepared by visual interpretation from remote sensing imagery collected by NOAA, 1999: https://data.noaa.gov/dataset/benthic-habitat-maps-of-the-u-s-virgin-islands-st-

15   thomas-and-st-john-prepared-by-visual-in-1999, last access: 22 Sept. 2016, 2001b.

Schlager, W.: The paradox of drowned reefs and carbonate platforms, Geological Society of American Bulletin, 92, 197-211, 1981.

Shalowitz, A. L.: Interpretation and Use of Nautical Charts, in: Shore and Sea Boundaries, U. S. Government Printing Office, Washington, DC, 269-355, 1964.

20   Sheppard, C., Dixon, D. J., Gourlay, M., Sheppard, A., and Payet, R.: Coral mortality increases wave energy reaching shores protected by reef flats: Examples from the Seychelles, Estuar. Coast. Shelf Sci., 64, 223-234, doi:10.1016/j.ecss.2005.02.016, 2005.

Shinn, E. A., Hudson, J. H., Halley, R. B., and Lidz, B.: Topographic control and accumulation rate of some Holocene coral reefs: south Florida and Dry Tortugas, Third International Coral Reef Symposium, Miami, Florida, 1977, 1-7, 1977.

25   Shinn, E. A., Reich, C. D., Hickey, T. D., and Lidz, B. H.: Staghorn tempestites in the Florida Keys, Coral Reefs, 22, 91-97, doi:10.1007/s00338-003-0289-2, 2003.

Stearn, C. W., Scoffin, T.P. & martinade, W.: Calcium carbonate budget of a fringing reef on the west coast of Barbados Part 1 - zonation and productivity, Journal of Marine Science, 27, 479-510, 1977.

Storlazzi, C. D., Elias, E., Field, M. E., and Presto, M. K.: Numerical modeling of the impact of sea-level rise on fringing

30   coral reef hydrodynamics and sediment transport, Coral Reefs, 30, 83-96, doi:10.1007/s00338-011-0723-9, 2011.

Taylor, K. H., and Purkis, S. J.: Evidence for southward migration of mud banks in Florida Bay, Mar. Geol., 311-314, 52-56, doi:10.1016/j.margeo.2012.04.007, 2012.

U.S. Army Corps of Engineers-JALBTCX: 1999 USACE Bathymetric LiDAR: Hawaiian Islands, NOAA Office for Coastal Management, Place Published,

http://www.coast.noaa.gov/htdata/lidar1_z/geoid12a/data/1457/1999_USACE_HI_Bathy_metadata.html, last access: 22 Sept. 2016, 1999.

U.S. Army Corps of Engineers-JALBTCX: Looe Key, Florida 2004 LiDAR coverage, USACE National Coastal Mapping Program Place Published, http://catalog.data.gov/dataset/looe-key-florida-2004-lidar-coverage-usace-national-coastal-mapping-program, last access: 22 Sept. 2016, 2004.

Census of Population and Housing http://www.census.gov/prod/www/decennial.html, last access: 22 Sept. 2016.

Table 1. Seafloor elevation and volume change for Atlantic, Pacific and Caribbean study sites. Minimum (Min.) and maximum (Max.) volumes are based on vertical error analysis (Table 4). Parenthetical numbers indicate number of combined habitat classes for each location (Tables 2 and 3). Mm^3 = millions of cubic meters.

Location, time period	Study area (km^2)	Mean elevation change (m)	Standard deviation (m)	Gross erosion (Mm^3)		Gross accretion (Mm^3)		Net change (Mm^3)	volume	Area- normalized volume change (Mm^3/km^2)	
				Min.	Max.	Min.	Max.	Min.	Max.	Min.	Max.
UFK, 1934/35-2002	241.1	-0.1	0.8	-22.2	-69.9	7.5	32.1	-14.6	-37.9	-0.06	-0.2
LFK, 1938-2004	19.0	-0.3	0.8	-1.8	-8.2	1.6	2.6	-0.2	-5.7	-0.01	-0.3
STT, 1966/73-2014	116.9	-0.3	0.9	-7.4	-29.1	1.4	7.5	-6.0	-21.6	-0.05	-0.2
BI, 1981/82-2014	51.8	-0.09	0.7	-2.3	-9.6	0.7	6.1	-1.6	-3.4	-0.03	-0.07
Maui, 1961/65-1999	84.5	-0.8	1.5	-56.6	-88.5	3.2	7.2	-52.8	-80.5	-0.6	-0.9
UFK coral habitats (5)	36.1	-0.2	1.1	-5.9	-14.3	2.3	6.3	-3.5	-7.9	-0.1	-0.2
UFK adjacent habitats	204.9	-0.1	-0.7	-15.6	-54.9	4.8	25.0	-10.8	-30	-0.05	-0.15
LFK coral habitats (4)	1.6	0.2	1.4	-0.1	-0.4	0.9	1.3	0.8	0.9	0.50	0.55
LFK adjacent habitats	17.3	-0.4	0.6	-1.6	-7.8	0.7	1.3	-1.0	-6.5	-0.06	-0.40
STT coral habitats (9)	14.3	-0.5	1.3	-4.0	-7.9	0.6	1.7	-3.4	-6.2	-0.2	-0.4
STT adjacent habitats	102.7	-0.2	0.6	-3.3	-21.2	0.7	5.8	-2.6	-15.4	-0.03	-0.2
BI coral habitats (7)	47.1	-0.09	0.72	-2.0	-8.7	0.6	5.6	-1.4	-3.1	-0.03	-0.07
BI adjacent habitats	4.7	-0.09	0.68	-0.3	-0.9	0.1	0.6	-0.2	-0.3	-0.05	-0.07
Maui coral habitats (7)	48.4	-0.9	1.5	-32.2	-50.0	1.9	4.2	-30.4	-45.8	-0.6	-0.9
Maui adjacent habitats	36.2	-0.8	1.5	-23.5	-37.3	1.1	2.6	-22.4	-34.7	-0.6	-1.0

Table 2. Elevation change by habitat type.

Location	Area (km²)	Total points (#)	Mean elevation change (m)	Stdev (m)	Max loss (m)	Max gain (m)	Elevation loss points (#)	Mean loss (m)	Stdev (m)	Elevation gain points (#)	Mean gain (m)	Stdev (m)
Upper Florida Keys												
Total study site	241.1	26341	-0.1	0.8	-8.3	6.5	14996	-0.6	0.7	11345	0.44	0.51
*Scattered coral/rock in uncons. sed.	0.2	17	-0.8	0.9	-2.0	1.2	13	-1.1	0.6	4	0.5	0.4
Pavement	17.0	1901	-0.2	1.0	-6.2	4.9	1218	-0.7	0.7	683	0.7	0.7
*Aggregate reef	11.8	1435	-0.2	1.1	-5.1	4.7	857	-0.8	0.8	578	0.7	0.7
*Reef rubble	1.5	291	-0.2	0.8	-2.6	3.2	196	-0.6	0.5	95	0.6	0.7
Unconsolidated sediments	65.3	5498	-0.2	0.6	-6.8	3.4	3526	-0.5	0.5	1972	0.3	0.3
*Individual or aggregate patch reef	17.2	2078	-0.2	1.1	-6.6	5.2	1170	-0.8	0.9	908	0.6	0.7
Seagrass continuous	63.5	6826	-0.2	0.8	-8.0	3.2	3604	-0.6	0.8	3322	0.4	0.3
Seagrass discontinuous	51.9	6944	-0.1	0.5	-8.3	2.6	3721	-0.4	0.4	3223	0.3	0.3
*Spur and groove	5.5	613	-0.02	1.3	-4.6	6.5	343	-0.8	0.8	270	1.0	1.0
Pavement w/sand channels	6.3	623	0.2	1.2	-3.2	5.7	313	-0.8	0.7	310	1.1	0.9
Not classified	0.7	113	0.2	0.5	-2.0	2.0	34	-0.4	0.4	79	0.4	0.3
Lower Florida Keys, Looe Key												
Total study site	19.0	1688	-0.3	0.8	-4.0	7.3	1361	-0.6	0.4	327	0.7	1.1
*Individual or aggregate patch reef	0.1	14	-0.8	0.8	-3.5	-0.2	14	-0.8	0.8	-	-	-
*Reef rubble	0.4	68	-0.7	0.8	-2.9	0.9	55	-0.9	0.6	13	0.3	0.3
Seagrass continuous	3.6	285	-0.5	0.4	-3.1	0.4	264	-0.5	0.3	21	0.2	0.1
Seagrass discontinuous	4.6	488	-0.5	0.5	-1.9	2.0	427	-0.6	0.3	61	0.3	0.3
Pavement	2.2	198	-0.4	0.7	-2.2	1.9	151	-0.6	0.4	47	0.5	0.5
Unconsolidated sediments	6.8	533	-0.4	0.7	-4.0	6.3	428	-0.6	0.4	105	0.7	1.0
*Spur and groove	0.7	68	0.5	1.1	-1.4	4.2	21	-0.5	0.4	47	1.0	1.0
*Aggregate reef	0.4	29	2.0	1.9	-1.4	7.3	1	-1.4	0.0	28	2.2	1.9
Not classified	0.1	5	3.0	1.3	0.7	4.1	-	-	-	5	2.9	1.3
St. Thomas, US Virgin Islands												
Total study site	116.9	49269	-0.3	0.9	-11.2	25.6	35332	-0.5	0.7	13937	0.4	0.9
*Spur and groove	0.1	75	-1.1	1.6	-5.9	3.1	60	-1.6	1.2	15	1.1	0.9
*Patch reef (aggregate)	0.4	163	-1.0	1.6	-5.9	4.9	138	-1.3	1.4	25	0.9	1.2
*Linear reef	4.2	2244	-0.7	1.5	-11.2	7.0	1632	-1.2	1.4	612	0.7	0.8
*Colonized bedrock	2.4	1968	-0.6	1.5	-8.3	6.1	1358	-1.2	1.2	610	0.9	1.0
*Colonized pave.w/sand channels	1.5	591	-0.5	1.0	-5.7	4.3	438	-0.9	0.8	153	0.5	0.6
Uncolonized pave. w/sand channels	0.1	41	-0.5	0.9	-3.0	0.9	27	-0.9	0.9	14	0.3	0.3
Mud	1.7	1857	-0.5	1.1	-5.6	3.4	1262	-1.0	0.9	595	0.5	0.5
*Scattered coral/rock in uncons. sed.	0.5	324	-0.5	1.3	-8.4	4.3	228	-0.9	1.2	96	0.5	0.7
*Colonized pavement	4.7	3195	-0.4	1.0	-7.9	8.1	2249	-0.8	0.9	946	0.5	0.6
*Patch reef (individual)	0.4	280	-0.3	1.1	-5.3	3.2	193	-0.8	0.8	87	0.7	0.8
Seagrass	16.0	11113	-0.2	0.6	-7.5	13.2	7914	-0.4	0.6	3199	0.3	0.5
Macroalgae	44.5	13973	-0.2	0.5	-11.1	4.0	10360	-0.3	0.5	3613	0.2	0.2
Sand	1.6	961	-0.2	0.8	-4.2	3.9	571	-0.6	0.6	390	0.4	0.5
Unknown	38.8	11992	-0.2	0.6	-8.6	11.5	8533	-0.3	0.5	3459	0.2	0.5
*Reef rubble	0.02	1	-0.1	0	-0.1	-	1	-0.1	0	-	-	-
Uncolonized pavement	0.1	33	-0.1	0.4	-1.2	0.7	20	-0.3	0.4	13	0.2	0.2
Uncolonized bedrock	0.02	6	1.1	1.0	-	2.3	-	-	-	6	1.1	1.0
Buck Island, US Virgin Islands												
Total study site	51.8	13894	-0.1	0.7	-8.6	6.8	7200	-0.5	0.7	6694	0.4	0.4
*Patch reef (aggregated)	3.2	1086	-0.5	1.5	-8.6	6.8	629	-1.3	1.5	457	0.5	0.9
*Patch reef (individual)	0.1	17	-0.3	0.5	-1.5	0.7	13	-0.5	0.4	4	0.3	0.3
Unknown	1.8	551	-0.3	0.9	-4.9	3.5	326	-0.8	0.8	225	0.5	0.5
*Colonized pave./w sand channels	27.3	6914	-0.1	0.6	-5.9	3.3	3809	-0.4	0.5	3105	0.3	0.3
*Scattered coral/rock in uncons. sed.	4.5	1152	-0.01	0.6	-4.7	2.8	490	-0.4	0.6	662	0.3	0.3
*Reef rubble	0.03	10	0	0.3	-0.5	0.5	5	-0.3	0.2	5	0.3	0.2
*Colonized pavement	11.9	3286	0.01	0.5	-3.0	4.5	1529	-0.4	0.4	1757	0.3	0.3
Seagrass	2.4	610	0.02	0.4	-2.2	0.9	270	-0.2	0.3	340	0.2	0.2
Sand	0.4	88	0.1	0.6	-3.8	0.9	27	-0.5	0.8	61	0.3	0.2
Macroalgae	0.1	26	0.2	0.5	-1.6	0.7	4	-0.6	0.7	22	0.3	0.2

*Linear reef	0.1	83	0.6	2.1	-3.0	5.7	43	-0.9	0.8	40	2.2	1.9
Maui, Hawaii											
Total study site	84.5	27518	-0.8	1.5	-28.7	11.8	22111	-1.2	1.4	5407	0.7	0.9
*Individual patch reef	0.1	166	-1.3	2.0	-7.4	4.9	140	-1.9	1.5	26	1.6	1.3
*Coral reef and hardbottom	19.5	5610	-1.3	2.0	-16.7	8.3	4592	-1.8	1.8	1018	1.0	1.2
Unknown	13.2	4548	-1.2	2.2	-28.7	9.2	3520	-1.8	2.1	1028	0.8	1.0
*Spur and groove	2.1	369	-0.8	1.1	-9.2	2.7	300	-1.1	1.0	69	0.5	0.5
*Aggregate patch reef	0.3	170	-0.7	0.8	-3.9	1.7	148	-0.9	0.7	22	0.6	0.5
*Aggregate reef	12.8	3666	-0.7	1.1	-9.4	8.6	2892	-1.0	0.9	774	0.6	0.8
Sand	22.5	8381	-0.6	0.8	-11.5	9.8	7272	-0.8	0.7	1109	0.5	0.7
*Scattered coral/rock	0.04	17	-0.6	0.7	-2.1	0.9	15	-0.7	0.5	2	0.7	0.3
*Coral pavement	13.5	4412	-0.4	0.9	-10.4	6.4	3120	-0.8	0.8	1292	0.5	0.6
Pavement w/sand channels	0.4	158	-0.4	0.9	-4.3	1.8	105	-0.8	0.8	53	0.5	0.4
Rubble	0.03	10	0.03	0.5	-0.5	0.8	5	-0.4	0.1	5	0.5	0.3
Mud	0.005	4	0.2	1.3	-0.6	2.1	3	-0.4	0.2	1	2.1	0.0

Notes: * = coral-dominated substrate. Uncons. sed. = unconsolidated sediment. Pave. = pavement. /w = with. Dashes indicate not applicable. Data points were excluded from habitat analysis where no habitat delineations were available. Total study site values include all data points.

Table 3. Volume change by habitat type

Location	Habitat area (km²)	Gross erosion (Mm³)		Gross accretion (Mm³)		Net volume change (Mm³/study area)		Area-normalized volume change (Mm³/km²)	
		Lower	Upper	Lower	Upper	Lower	Upper	Lower	Upper
Upper Florida Keys									
Total study site	241.1	-21.5	-69.2	7.1	31.3	-14.3	-37.9	-0.1	-0.2
*Scattered coral/rock in uncons. sed.	0.2	-0.1	-0.1	0.00	0.01	-0.1	-0.1	-0.3	-0.7
Pavement	17.0	-2.4	-6.6	0.8	2.4	-1.6	-4.3	-0.1	-0.3
*Aggregate reef	11.8	-1.9	-4.5	0.8	2.3	-1.1	-2.2	-0.1	-0.2
*Reef rubble	1.5	-0.2	-0.6	0.1	0.2	-0.1	-0.4	-0.1	-0.2
Unconsolidated sediments	65.3	-4.1	-17.5	0.9	5.8	-3.2	-11.7	-0.05	-0.2
*Individual or aggregate patch reef	17.2	-2.9	-7.1	0.6	2.1	-2.4	-4.9	-0.1	-0.3
Seagrass continuous	63.5	-6.4	-18.7	1.1	8.5	-5.2	-10.2	-0.1	-0.2
Seagrass discontinuous	51.9	-2.0	-9.8	0.7	6.0	-1.3	-3.9	-0.02	-0.1
*Spur and groove	5.5	-0.8	-2.0	0.8	1.6	0.1	-0.3	0.01	-0.1
Pavement with sand channels	6.3	-0.8	-2.2	1.2	2.2	0.4	-0.04	0.1	-0.01
Not classified	0.7	-0.01	-0.04	0.03	0.2	0.02	0.1	0.03	0.2
Lower Florida Keys, Looe Key									
Total study site	19.0	-1.7	-8.2	1.6	2.6	-0.1	-5.6	-0.01	-0.3
*Individual or aggregate patch reef	0.1	-0.02	-0.1	0.00	0.00	-0.02	-0.1	-0.2	-0.6
*Reef rubble	0.4	-0.1	-0.2	0.00	0.01	-0.1	-0.2	-0.2	-0.5
Seagrass continuous	3.6	-0.2	-1.7	0.00	0.01	-0.2	-1.7	-0.1	-0.5
Seagrass discontinuous	4.6	-0.5	-2.3	0.0	0.1	-0.5	-2.2	-0.1	-0.5
Pavement	2.2	-0.2	-0.9	0.02	0.1	-0.2	-0.8	-0.1	-0.3
Unconsolidated sediments	6.8	-0.7	-2.9	0.5	0.9	-0.2	-2.0	-0.02	-0.3
*Spur and groove	0.7	-0.01	-0.1	0.2	0.4	0.2	0.3	0.3	0.4
*Aggregate reef	0.4	0.00	-0.01	0.7	0.9	0.7	0.9	1.6	2.1
Not classified	0.1	0.00	0.00	0.1	0.2	0.1	0.2	1.7	2.2
St. Thomas, US Virgin Islands									
Total study site	116.9	-7.4	-29.1	1.4	7.5	-6.0	-21.6	-0.05	-0.2
*Spur and groove	0.1	-0.1	-0.2	0.00	0.01	-0.1	-0.2	-0.8	-1.2
*Patch reef (aggregate)	0.4	-0.2	-0.3	0.00	0.02	-0.2	-0.3	-0.4	-0.7
*Linear reef	4.2	-1.3	-2.4	0.2	0.5	-1.1	-1.9	-0.3	-0.5
*Colonized bedrock	2.4	-1.0	-1.8	0.2	0.4	-0.8	-1.3	-0.3	-0.6
*Colonized pavement with sand channels	1.5	-0.3	-0.8	0.02	0.1	-0.3	-0.7	-0.2	-0.5
Uncolonized pavement with sand channels	0.1	0.0	-0.1	0.00	0.01	-0.02	-0.05	-0.2	-0.5
Mud	1.7	-0.6	-1.0	0.1	0.3	-0.5	-0.8	-0.3	-0.5
*Scattered coral/rock in uncons. sed.	0.5	-0.1	-0.2	0.02	0.1	-0.1	-0.1	-0.2	-0.3
*Colonized pavement	4.7	-0.9	-2.0	0.2	0.5	-0.8	-1.5	-0.2	-0.3
*Patch reef (individual)	0.4	-0.1	-0.2	0.02	0.1	-0.1	-0.2	-0.2	-0.4
Seagrass	16.0	-0.9	-3.6	0.1	0.9	-0.7	-2.7	-0.05	-0.2
Macroalgae	44.5	-1.1	-9.8	0.1	1.9	-1.0	-8.0	-0.02	-0.2
Sand	1.6	-0.1	-0.4	0.03	0.1	-0.1	-0.3	-0.1	-0.2
Unknown	38.8	-0.6	-6.2	0.3	2.6	-0.2	-3.6	-0.01	-0.1
*Reef rubble	0.02	0.00	-0.01	0.00	0.00	0.00	-0.01	-0.1	-0.5
Uncolonized pavement	0.1	0.00	-0.01	0.00	0.01	0.00	0.00	-0.02	0.0
Uncolonized bedrock	0.02	0.00	0.00	0.00	0.01	0.00	0.01	0.2	0.3
Buck Island, US Virgin Islands									
Total study site	51.8	-2.3	-9.6	0.7	6.1	-1.6	-3.4	-0.03	-0.07
*Patch reef (aggregated)	3.2	-0.9	-1.6	0.1	0.4	-0.8	-1.2	-0.2	-0.4
*Patch reef (individual)	0.1	0.00	-0.01	0.00	0.00	0.00	-0.01	-0.03	-0.2
Unknown	1.8	-0.2	-0.6	0.05	0.2	-0.2	-0.4	-0.1	-0.2
*Colonized pavement with sand channels	27.3	-0.8	-5.0	0.3	2.9	-0.5	-2.1	-0.02	-0.1
*Scattered coral/rock in uncons. sed.	4.5	-0.1	-0.5	0.00	0.6	-0.1	0.0	-0.01	0.01
*Reef rubble	0.03	0.00	-0.01	0.00	0.00	0.00	0.00	-0.03	-0.1
*Colonized pavement	11.9	-0.2	-1.4	0.1	1.6	-0.02	0.2	0.00	0.01
Seagrass	2.4	-0.03	-0.2	0.00	0.2	-0.02	0.1	-0.01	0.0

Sand	0.4	-0.01	-0.04	0.01	0.07	0.00	0.02	-0.01	0.1
Macroalgae	0.1	0.00	-0.01	0.00	0.02	0.00	0.00	-0.02	0.0
*Linear reef	0.1	-0.01	-0.03	0.04	0.05	0.02	0.02	0.4	0.3
Maui, Hawaii									
Total study site	84.5	-55.8	-87.2	3.0	6.7	-52.8	-80.5	-0.6	-1.0
*Individual patch reef	0.1	-0.1	-0.1	0.01	0.01	-0.1	-0.1	-0.9	-1.2
*Coral reef and hardbottom	19.5	-23.3	-31.4	1.1	1.9	-22.2	-29.4	-1.1	-1.5
Unknown	13.2	-15.0	-19.9	0.7	1.5	-14.2	-18.3	-1.1	-1.4
*Spur and groove	2.1	-0.9	-1.7	0.03	0.1	-0.8	-1.6	-0.4	-0.8
*Aggregate patch reef	0.3	-0.1	-0.2	0.00	0.02	-0.1	-0.1	-0.2	-0.5
*Aggregate reef	12.8	-4.7	-9.4	0.3	0.8	-4.4	-8.7	-0.3	-0.7
Sand	22.5	-8.5	-17.2	0.3	1.0	-8.2	-16.2	-0.4	-0.7
*Scattered coral/rock	0.04	-0.01	-0.03	0.00	0.00	-0.01	-0.03	-0.3	-0.7
*Coral pavement	13.5	-3.2	-7.2	0.4	1.3	-2.8	-5.8	-0.2	-0.4
Pavement with sand channels	0.4	-0.1	-0.2	0.01	0.1	-0.1	-0.2	-0.2	-0.3
Rubble	0.03	0.00	0.00	0.00	0.01	0.00	0.00	0.01	0.1
Mud	0.005	0.00	0.00	0.00	0.00	0.00	0.00	0.02	-0.04

* = coral-dominated substrate.

5   **Table 4.** Vertical error-analysis results.

Study site	Historical Data			Modern Data	VDatum	Study Site Totals	
	# paired points	RMSE$_{Sounding}$ (m)	T-test results (±, P)	RMSE$_{Lidar}$ (m)	RMSE$_{VDatum}$ (m)	RMSE$_{Total}$ (m)	*1.65 x study site RMSE$_{Total}$ (m)
UFK	38	0.23	+, 0.96	0.15	0.081	0.29	0.47
STT	184	0.26	+, 0.81	0.135	0.114	0.31	0.52
STC	29	0.32	+, 0.93	0.135	0.114	0.37	0.60
Maui	46	0.13	+, 0.99	0.15	-	0.20	0.33
Average	-	-	-	-	-	0.29	0.48

Notes: LFK was excluded from the error analysis because no adjacent points were separated by 0.5 m or less.

For t-test results, + = accept H$_0$. *1.65 x study site RMSE$_{Total}$ = 90% of variance.

5 **Table 5.** Horizontal shift analysis results. Un-shifted results are derived from the original point to DEM data sets, correctly aligned to horizontal datums, for each study site. Experimental data sets were created by shifting UTM northings and eastings of historical elevation XYZ data sets by plus or minus 10 m and recalculating volume change relative to unshifted LiDAR elevation data.

Study site & relative location	Net volume change (Mm^3)	% difference from un-shifted value	Area- normalized volume change (Mm^3/km^2)	% difference from un-shifted value
UFK				
Un-shifted	-37.9	-	-0.16	-
x + 10 m	-41.7	10	-0.17	6
x − 10 m	-34.9	8	-0.15	6
y + 10 m	-36.6	3	-0.15	6
y − 10 m	-39.5	4	-0.16	0
LFK				
Un-shifted	-5.7	-	-0.30	-
x + 10 m	-5.8	2	-0.31	3
x − 10 m	-5.4	5	-0.29	3
y + 10 m	-4.5	21	-0.24	20
y − 10 m	-6.7	18	-0.35	17
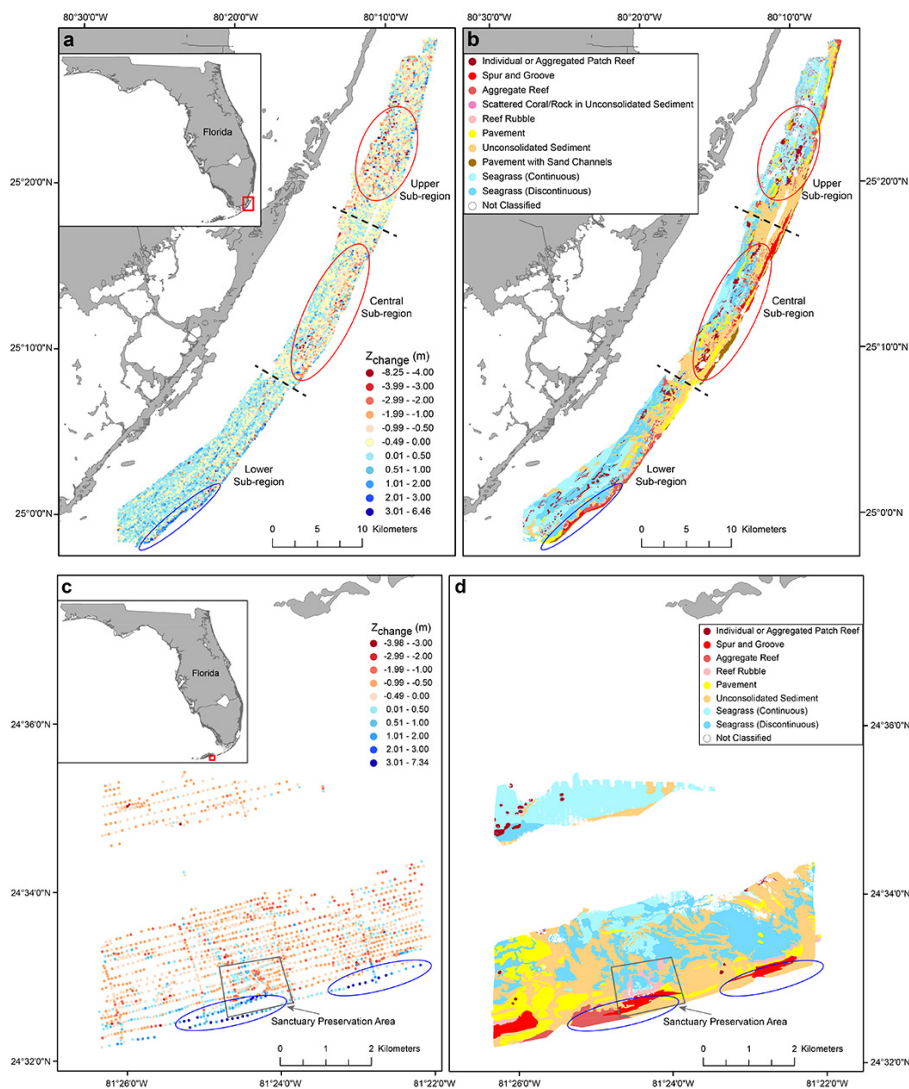
Figure 1. Elevation-change and habitat maps for the Upper Florida Keys (a and b) and Lower Florida Keys (c and d) over 68 and 66 years, respectively. Elevation values are differences in meters between modern and historical elevation data (Z_{change} = modern elevation – historical elevation, see Tables S4 and S5). Negative numbers indicate elevation loss, positive numbers indicate elevation gain. Red and blue circles indicate areas of high erosion and accretion rates, respectively. Dashed lines = sub-regions. Habitat maps were modified from existing geo-databases (Table S1).
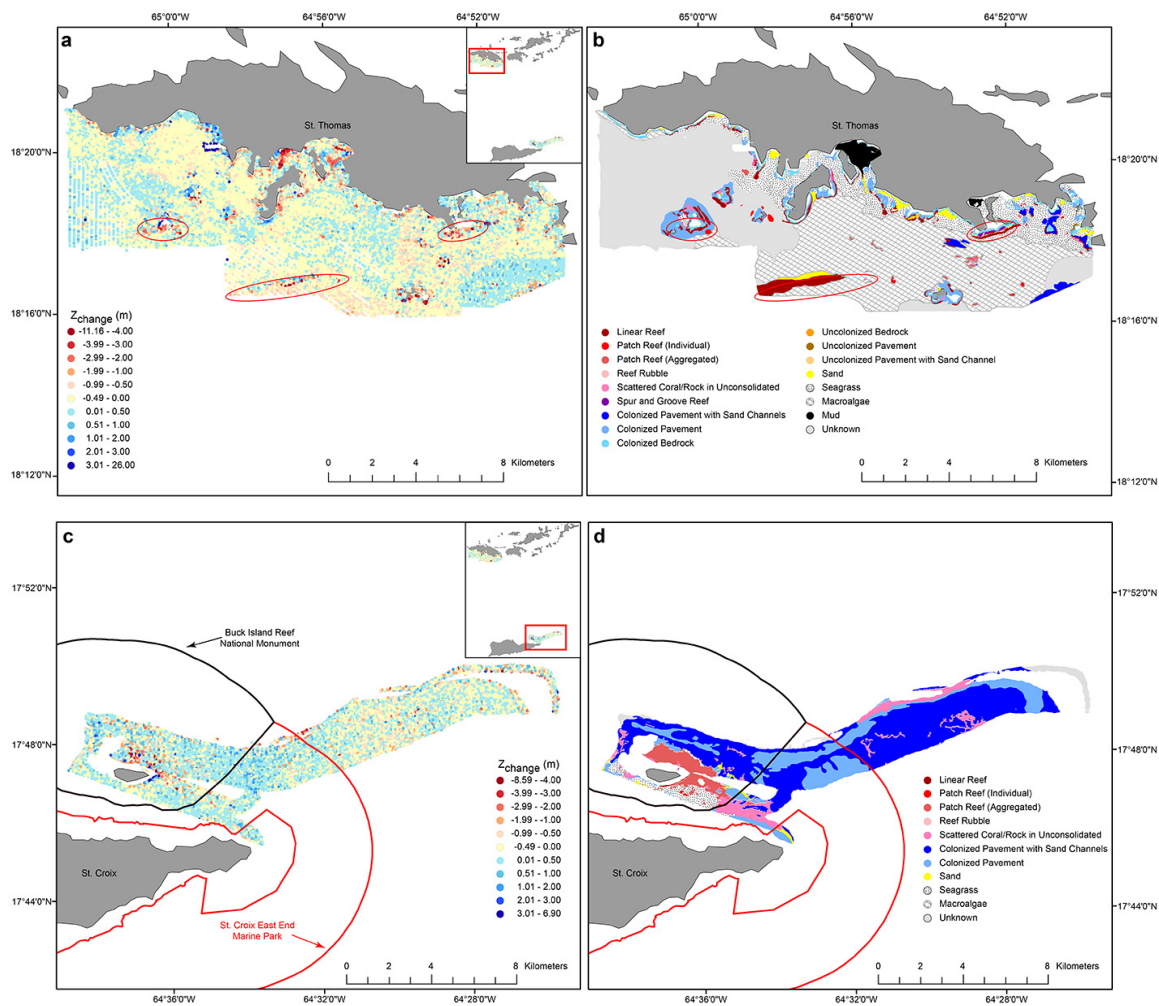
Figure 2. Elevation-change and habitat maps for the U.S. Virgin Islands. St. Thomas elevation-change over 48 years (a) and habitat (b). Buck Island elevation-change over 33 years (c) and habitat (d). Elevation values are differences in meters between modern and historical elevation data (Z_{change} = modern elevation – historical elevation, see Tables S6 and S7). Negative numbers indicate elevation loss, positive numbers indicate elevation gain. Red circles indicate areas of high erosion rates. Habitat maps were modified from existing geo-databases (Table S1).
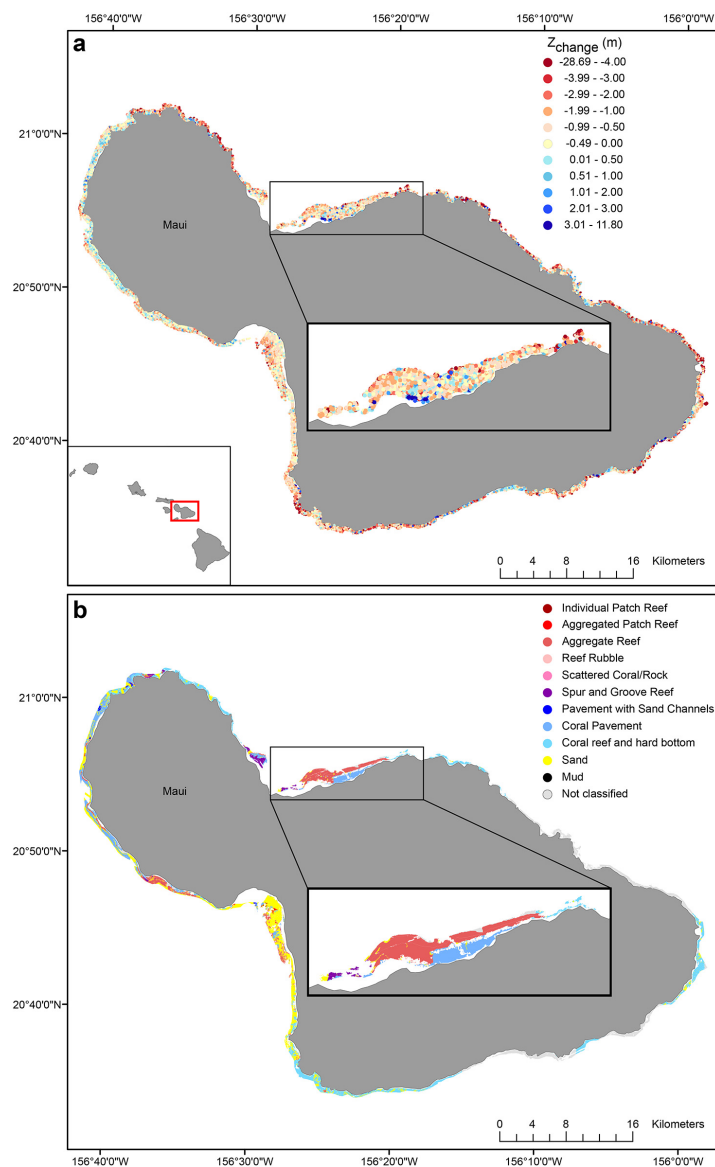
Figure 3. Elevation-change and habitat maps for Maui, Hawaii. Elevation-change over 38 years (a). Habitat (b). Elevation values are differences in meters between modern and historical elevation data (Z_{change} = modern elevation – historical elevation, see Table S8). Inset shows magnified detail of the north central reef tract. Negative numbers indicate elevation loss, positive numbers indicate elevation gain. Habitat maps were modified from existing geo-databases (Table S1).
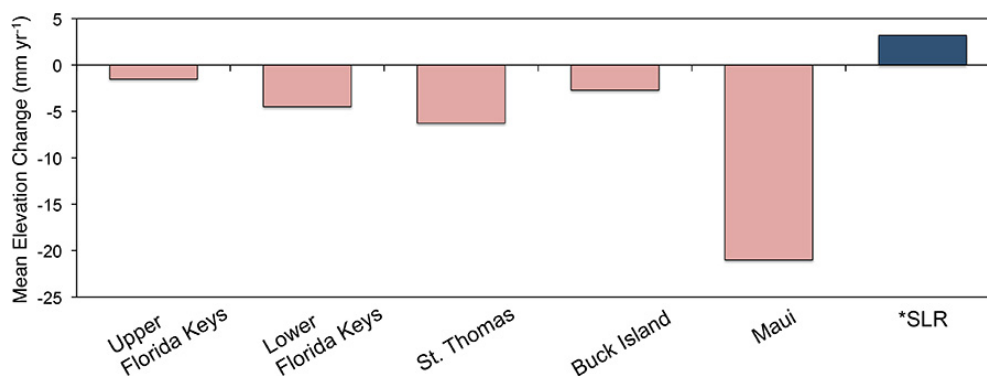
5 **Figure 4.** Mean annual elevation change calculated from total mean elevation change in meters (Table1) divided by the time range of historical to modern bathymetric data sets for each study site (Table S1). *SLR = global mean sea level rise of 3.2 mm yr^{-1}.
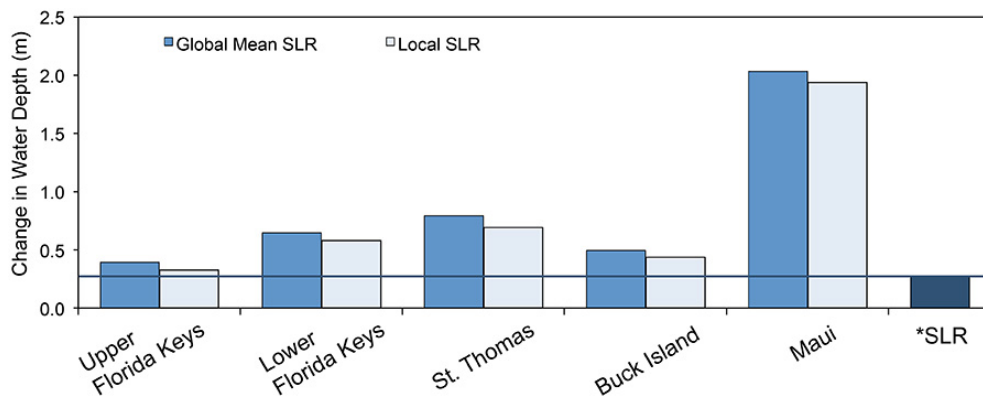
5   **Figure 5.** Projected water depth for the year 2100. Projected change in water depth by 2100 from combined impact of mean

rates of seafloor elevation loss and rising sea level based on local (a) NOAA sea-level rise trends downloaded on August 4,

2016 (http://tidesandcurrents.noaa.gov/products.html) and global sea level rise trends (b), see Table S9. *SLR = water depth

due only to global mean sea level rise of 3.2 mm yr^{-1}.